

**Spiking sugar neurons modulate dopaminergic neuron activity -
A study using a leaky Integrate-and-fire computational model
based on the entire adult Drosophila brain connectome**

**Dissertation Submitted for
the Partial Fulfilment
for the Award of
Master of Science
in
Bioinformatics**

by

Sharvani Togata

Regd. No: 22mslsbf03

**Under the Supervision of
Dr. Gaurav Das**

Co-Supervisor

Dr. Saraboji Kadhivel

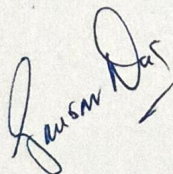


**DEPARTMENT OF COMPUTATIONAL SCIENCES
SCHOOL OF BASIC SCIENCES
CENTRAL UNIVERSITY OF PUNJAB, BATHINDA
JUNE – 2024**

CERTIFICATE

This is to certify that the dissertation entitled "How spiking sugar neurons modulate dopaminergic neuron activity - a study using a leaky integrate-and-fire computational model based on the entire adult Drosophila brain connectome" (topic of research) being submitted by Sharvani Togata (Name of Student), Registration No: 22mslsbf03 to Central University of Punjab, Bathinda for the award of Master's degree in the M.Sc.Bioinformatics, (discipline/subject) is a bonafide research work carried out by her/him under my supervision. The results presented in this dissertation have not been submitted elsewhere for the award of any other degree.

In my opinion, the dissertation work has reached the standard of fulfilling the requirements for the award of Master's degree in accordance with the regulations of Central University of Punjab, Bathinda.



7.6.24

(Signature of Supervisor)

Dr. Gaurav Das,
Scientist 'E'
National Centre for Cell Sciences
Pune
Date: 7.6.24.



(Signature of Co-Supervisor)

Dr. Saraboji Kadhivel
(Associate Professor & Head)
Department Of Computational sciences
Central University of Punjab
Date:

डॉ. गौरव दास / Dr. Gaurav Das
वैज्ञानिक 'ई' / Scientist 'E'
राष्ट्रीय कोशिका विज्ञान केंद्र, पुणे
National Centre for Cell Science, Pune

This is to certify that Ms. Sharvani Togata, student of MSc. Bioinformatics of Central University of Punjab, Bathinda, has successfully completed her fourth semester dissertation on report entitled "Spiking sugar neurons modulate dopaminergic neuron activity - A study using a leaky integrate-and-fire computational model based on the entire adult Drosophila brain connectome" at National Centre for Cell Science from 5-2-2024 to 14-6-2024. under the guidance of Dr. Gaurav Das, Scientist 'E',
National Centre for Cell Science, Pune

During this internship program with us, she had been exposed to different aspects of Drosophila Neuroscience and bioinformatics and was found to be punctual, sincere and hardworking.

डॉ. गौरव दास / Dr. Gaurav Das
वैज्ञानिक 'ई' / Scientist 'E'
राष्ट्रीय कोशिका विज्ञान केन्द्र, पुणे
National Centre for Cell Science, Pune

(Signature of Supervisor)

Dr. Gaurav Das,

Scientist 'E',

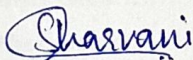
National Centre for Cell Science, Pune

DECLARATION

I, Sharvani Togata , Regd. No.22mslsbf03, of the Department of Computational Sciences declare that this dissertation is based on original ideas and free from plagiarism. Adequate citations and references of original sources have been provided.

I also declare that I have adhered to all principles of academic honesty and integrity and have not misinterpreted or fabricated or falsified any idea/data/fact/source in the dissertation.

I understand that any violation of the above will be the cause for disciplinary action by the Central University of Punjab and can also evoke penal action from the sources which have, thus, not been properly cited or from whom proper permission has not been taken when needed.



(Signature of the Student)

Registration No.: 22mslsbf03

Department of computational sciences

Date: 21.06.2024

CONTENTS

Page No

| | |
|---|-------|
| Acknowledgement..... | 4 |
| Abbreviations..... | 5 |
| List of Tables..... | 6 |
| List of Figures..... | 7 |
| 1. Abstract..... | 9 |
| 2. Introduction..... | 10-22 |
| 2.1. Drosophila as a model organism..... | 10 |
| 2.2. Drosophila connectome..... | 10-11 |
| 2.3. Flywire..... | 11 |
| 2.4. Mushroom Body..... | 12-15 |
| 2.5. Gustatory receptor neurons..... | 16 |
| 2.6. Leaky integrate and fire model..... | 16-21 |
| 2.7. Objectives..... | 22 |
| 3. Methodology | 23-25 |
| 4. Results..... | 26-39 |
| 4.1. Spiking PPL1-γ1pedc from 0 to 200 Hz..... | 26-29 |
| 4.2. Spiking PAM-β'2a FROM 0 to 200 Hz..... | 30-32 |
| 4.3. Spiking Sugar Neurons..... | 33-36 |
| 4.4. Spiking Sugar as well as dopaminergic neurons..... | 37-39 |
| 5. Discussion and conclusion | 40-41 |
| 6. Future work | 42 |
| 7. References..... | 43-46 |

ACKNOWLEDGMENT

I want to take this opportunity to acknowledge and express my heartfelt gratitude to all those who supported and guided me during my dissertation work. First and foremost, I thank my Supervisor, Dr. Gaurav Das, for allowing me to work on this topic and providing invaluable guidance and support throughout the research process. I thank my co-supervisor, Dr. Saraboji Kadhivel, for his unwavering support and cooperation. I also wish to thank Philip Shiu for the insightful discussions that have significantly contributed to my understanding and progress. Thanks to Ph.D. scholar Radhika Mohandasan for her help. I thank Piyush R. Maharana, Vipul Garg, and Kushal Vala for their constant help and support. I would like to express my gratitude to my family for their unconditional support and encouragement. I thank all my lab mates from The Brain and Feeding Behaviour Lab at the National Centre for Cell Science, Pune. I thank my friends for their support and understanding during this demanding period. Thank you all for your contributions to this work.

ABBREVIATIONS

1. MB- Mushroom body
2. EM- Electron Microscopy
3. FAFB- Full adult Fly brain
4. Ach- Acetylcholine
5. Glu- glutamate
6. GABA-
7. DA- Monoamines dopamine
8. Oct- Octopamine
9. Ser- Serotonin
10. KCs- Kenyon cells
11. MBONs- Mushroom body output neurons
12. DANs- Dopaminergic neurons
13. PAM- Protocerebral anterior medial cluster
14. PPL- Protocerebral posterior lateral clusters
15. C- Capacitance
16. R- Membrane resistance
17. LIF- leaky integrate and fire model
18. VNC- Ventral nerve cord
19. DN- descending neurons

LIST OF TABLES

Page No

| | |
|---|----|
| Table 1: Root-ids of set of PPL1- γ 1pedc activated. ----- | 26 |
| Table 2: Root-ids of a set of MBON11 that was activated after activation of PPL1- γ 1pedc showing connectivity between them----- | 27 |
| Table 3: Root-ids of set of PAM- β '2a activated----- | 30 |
| Table 4: Root-ids of a set of MBONs that were activated after activation of PAM- β '2a showing connectivity between them----- | 31 |
| Table 5: Root-ids of sugar neurons that were activated ----- | 35 |

LIST OF FIGURES

| | Page no |
|--|---------|
| Figure 1: Hierarchical annotation framework devised for the FlyWire Dataset..... | 12 |
| Figure 2: The MB lobes are divided into compartments. Projection neurons from the antennal lobe transmit olfactory information to the MB calyx, where they synapse on KCs. KC axons form the lobes, terminating on MBON dendrites, which intersect with DAN terminals in specific compartments. PPL1 and PAM DAN axon clusters, marked by dashed rectangles, with arrow size indicating memory strength..... | 13 |
| Figure 3 : Sensory input into KCs and how it gives behavioural responses as output | 15 |
| Figure 4: Connectivity between KCs, MBONs and DANs..... | 15 |
| Figure 5: circuit representation of biological neuron..... | 17 |
| Figure 6 : Diagram of the LIF..... | 21 |
| Figure 7: PPL1- γ 1pedc; a DAN of the PPL1 cluster with terminals that overlap with the dendrites of MBON- γ 1pedc α/β | 26 |
| Figure 8 : Heatmap depicting the predicted firing rates of MBONs in response to unilateral 0 to 200 Hz PPL1- γ 1pedc firing. The y-axis depicts the MBON IDs..... | 28 |
| Figure 9 : Lineplot depicting the predicted firing rate of two MBON11 ids X axis- depicts the PPL1- γ 1pedc firing rate from 0 to 200 Hz and y axis depicts the predicted firing rate of PPL1- γ 1pedc..... | 29 |
| Figure 10: Figures representing PAM- β '2a neurons, MBO-01 and MBON-03 neurons..... | 31 |

| | |
|---|----|
| Figure 11: Heatmap showing firing rates of MBONs in response to activation of PAM- β '2a unilateral 0 to 200 Hz . The y-axis depicts the MBON IDs , and x-axis depicts the activation of PAM- β '2a from 0 to 200 Hz..... | 32 |
| Figure 12: GRN R4#16 (FAFB:14928124) [VFB_00102914] visualized in VFB... | 33 |
| Figure 13: PAM-b'2(c1)#1_R (FAFB:8317886) [VFB_00101418] Visualised in VFB..... | 34 |
| Figure 14: The reconstructed circuitry between sugar sensing gustatory neuron and PAMB`2 using VFB circuit browser..... | 34 |
| Figure 15 : Simplified pathway depiction between sugar gustatory and motor system..... | 36 |
| Figure 16: PPL1-y1_R (FAFB:6893931) [VFB_001014ie] DAN PPL1-y1 Right 6893932 JS MWP visualised in VFB..... | 37 |
| Figure 17 : The heatmap displays the predicted activation rate (color scale on the right) as a function of two variables: the firing rate of PPL1-y1pedc neurons (y-axis) ranging from 0 to 200 Hz and the firing rate of Sugar GRN (gustatory receptor neurons) (x-axis) ranging from 0 to 200 Hz..... | 38 |

1.ABSTRACT

Obesity, affecting over 650 million individuals, underscores the critical need to understand the neurobiological mechanisms underlying dietary behaviours, particularly those driven by high-calorie, sugar-rich foods. This study explores the modulation of dopaminergic neuron activity by sugar neurons, using *Drosophila melanogaster* as a model organism. With its comprehensive connectome and intricate neural circuits, the highly developed *Drosophila* brain provides a unique opportunity to investigate the reward system and associative learning mechanisms. MB, a key centre for processing and storing associative memories, receives input from DANs and plays a crucial role in transforming sensory information into behavioural responses.

We utilize the FlyWire connectome, the most extensive *Drosophila* brain connectome to date, encompassing 127,978 neurons and approximately 16.5 million synaptic connections. By employing LIF model, we simulate the impact of sugar neuron spiking on the activity of specific DAN subsets involved in reward and aversion. This computational approach uses neuronal connectivity to predict changes in dopaminergic firing patterns. Our methodology involves stimulating sugar neurons and analysing the consequent modulation of DAN activity, providing insights into the neural basis of reward processing and decision-making.

This research aims to enhance our understanding of how dietary behaviours are encoded in the brain and offers a framework for studying neural mechanisms of reward and aversion. The findings have potential implications for developing interventions to address obesity and related disorders by targeting specific neural pathways involved in reward processing.

2. INTRODUCTION:

Over 650 million people worldwide suffer from obesity, resulting from consuming too many high-calorie, typically sugar-rich meals which causes the production of dopamine, a neurotransmitter linked to reward, in both insects and mammals. The act of seeking and eating sweets is reinforced by this dopamine release thus modulation of dopaminergic neuron activity by sugar neurons needs to be studied [1].

2.1. DROSOPHILA AS A MODEL ORGANISM:

The *Drosophila* brain is highly developed and features a prominent mushroom body (MB), which plays a crucial role in associative learning. Despite its complexity, the *Drosophila* brain remains sufficiently simple for comprehensive study. The fundamental concept behind investigating the reward system in *Drosophila* is that the fly can distinguish between rewarding and aversive stimuli. This ability is essential for associative learning and memory formation, driven by reward and punishment mechanisms [2].

2.2. DROSOPHILA CONNECTOME:

The intricate networks of neurons and their interconnections constitute the brain's structure. Analysing these networks using network theory can yield significant insights into the brain's computational abilities and information flow management mechanisms. The *Drosophila* connectome offers a distinctive opportunity to thoroughly investigate its network properties and topological features [3].

The adult fruit fly stands at the forefront of whole brain connectomics. With 127,978 neurons, (version v630 as of April 2023) the recently completed connectome of the adult female brain occupies an intermediate position on the logarithmic scale, between the initial *C. elegans* connectome (302 neurons) and that of the mouse (10^8 neurons). The complete connectome of the adult fly brain now enables the mapping of brain-wide circuits and their linkage to

circuit dynamics and behaviour. The adult fruit fly exhibits a range of sophisticated behaviours, including complex motor control during walking and flight, courtship behaviours, decision making, flexible associative memory, spatial learning, and intricate multisensory navigation [4].

2.3. FLYWIRE :

The FlyWire connectome represents the most extensive and intricate connectome achieved to date. This complete connectome, derived from the approximately 100-teravoxel FAFB whole-brain EM volume, can be depicted as a graph containing 127,978 nodes and around 16.5 million weighted edges [4]. Sections of fly brains have been reconstructed from EM images, which offer sufficient resolution to reveal the intricate branching of neurons and the synapses connecting them [5].

An edge consisting of one or more synapses between two neurons in a network is referred to as a "connection". Neurotransmitter synapse-level predictions are also included in the Fly-Wire connectome [6]. Six neurotransmitters are classified by the classifier used to this dataset: DA, Oct, Ser , and the fast-acting classical neurotransmitters Ach, Glu, and GABA. Ach functions as an excitatory neurotransmitter and GABA as an inhibitory neurotransmitter in the nervous system of *Drosophila*. Although glutamate has excitatory and inhibitory properties, it is mostly shown to have an inhibitory effect on the fly's brain [7, 8, 9].

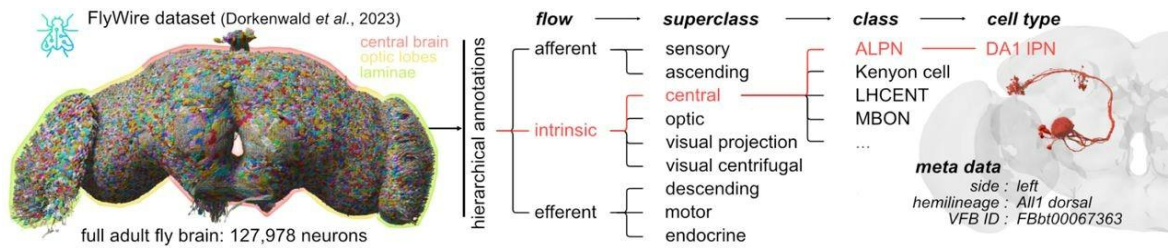


Figure 1: Hierarchical annotation framework devised for the FlyWire dataset [4,5].

2.4. MUSHROOM BODY:

MB in the *Drosophila* brain serves as a central hub responsible for the processing and retention of associative memories, while also playing a crucial role in the integration of sensory cues. It is made up of various types of neurons that are carefully put together during development. These neurons include KCs and MBONs, along with DANs.

MB lobes are densely populated by extrinsic neurons, mainly DANs and MBONs [10, 3, 11]. Around 2000 KCs project to the MB lobes, providing inputs to both MBONs and DANs. There are 34 MBONs of 21 different types and approximately 130 DANs, which are classified into 20 types within two families: PAM and PPL1 [3]. The MB receives input from primary sensory centres and forms three lobes. These lobes are innervated by the axons of DANs originating from the PPL1 and PAM clusters, which convey aversive and appetitive stimuli, respectively [12, 13, 14, 15, 16].

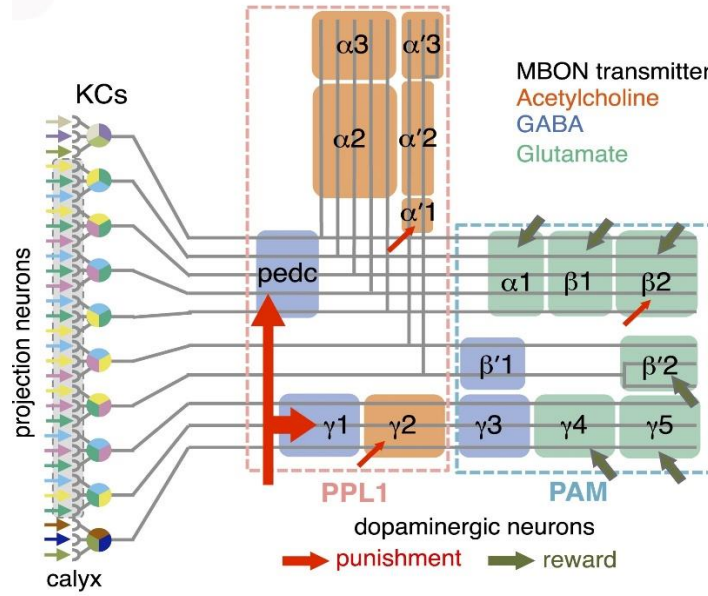


Figure 2 : The MB lobes are divided into compartments. Projection neurons from the antennal lobe transmit olfactory information to the MB calyx, where they synapse on KCs. KC axons form the lobes, terminating on MBON dendrites, which intersect with DAN terminals in specific compartments. PPL1 and PAM DAN axon clusters, marked by dashed rectangles, with arrow size indicating memory strength. [3]

The compartments of the MB lobes are organized to receive inputs from KCs and specific DANs, which then send information to a specific set of MBONs. Each compartment is influenced by unique dopaminergic inputs that can change the synapses between KCs and specific MBONs. These compartments might act as basic computational units within the MB. Dopaminergic inputs are crucial for turning the random KC representation of stimuli into a structured MBON representation that reflects behavioral tendencies. Different groups of DANs respond to various environmental features [17, 16, 18, 19].

DANs project their axons into the mushroom body (MB), functioning as the primary afferent neurons responsible for conveying signals related to reinforcement and physiological state to the lobes of the MB [20].

Learning consists of modulation of DAN activity to influence MBON activity, thereby constructing a model that anticipates the consequences of a given stimulus [3].

The arrangement of MBON and DAN dendrites and axons indicates that the MB lobes have both feedforward and feedback circuits. MBON interactions form a multi-layer feedforward network, boosting the brain's computing power and enabling more advanced learning techniques. This layered MBON network structure allows for updating and adjusting past learning experiences [3].

The dendrites of DANs and the axons of MBONs overlap in most of the MBON projection zones, suggesting that MBONs can affect DAN activity, forming a feedback loop. After response is acquired, this loop may provide negative feedback to decrease dopamine release or positive feedback to improve learning for significant stimuli. These connections also allow the output from one compartment to affect learning in other compartments since some MBONs target DANs that connect to different compartments [3].

Sensory cues are encoded by specific subsets of cholinergic Kenyon cells (KCs), projecting to MBONs of roughly 21 types utilizing different neurotransmitters, which promote approach or repulsion behaviours. Dopamine release during learning modulates KC-MBON connections, influencing the overall output network and behavioural responses [21].

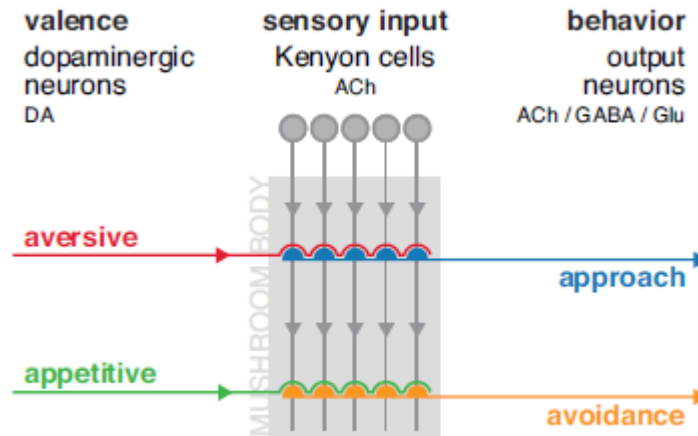


Figure 3 : Sensory input into KCs and how it gives behavioural responses as output [21].

Microcircuits within compartments involve KCs, MBONs, and DANs, with KC to DAN connections likely modulating the dopaminergic reinforcement signal. DANs synapse onto KCs and MBONs, potentially facilitating a local excitatory feedback loop. Feedback architecture is observed consists of three synapses, where KCs, DANs, and MBONs interact bidirectionally. This structure helps in creating a robust learning and memory system by allowing for dynamic and flexible modulation of neural activity [21].

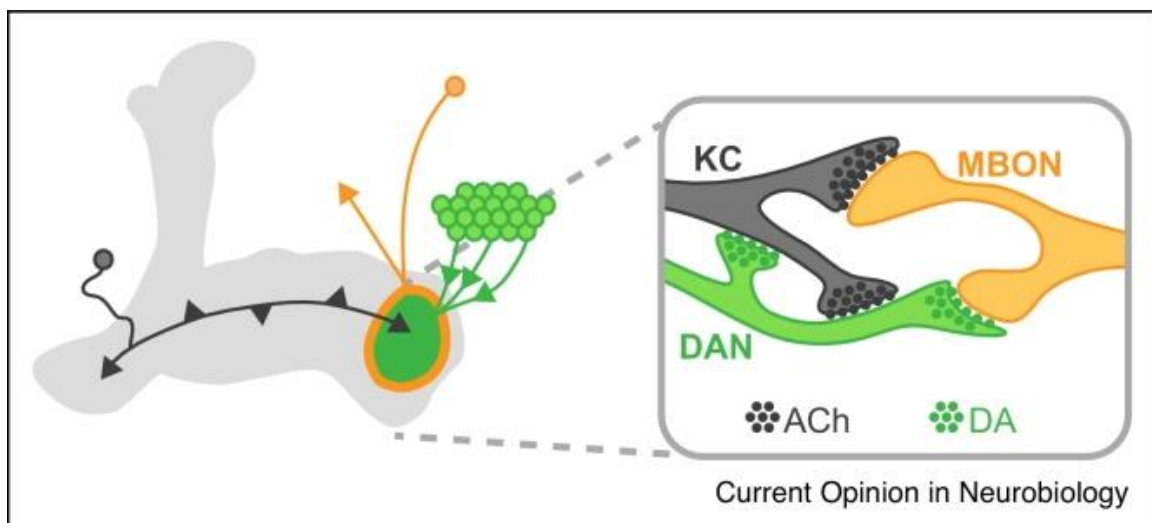


Figure 4: Connectivity between KCs, MBONs and DANs [21]

2.5. GUSTATORY RECEPTOR NEURONS:

Fruit fly gustatory receptors (GRs) are a class of receptors in the fruit fly labellum are divided into five categories according to their unique receptor profiles and responses to different taste modalities: "sweet," "bitter," "sour," "salty," and "umami" (Jaeger et al., 2018). These five GRN types can be reliably identified on the labellum of a fly (Falk et al., 1976; Freeman & Dahanukar, 2015; Stocker, 1994).

When a fly encounters attractive food sources like sugar, its gustatory receptor neurons (GRNs) on the proboscis activate the proboscis extension reflex (PER). This reflex causes the proboscis to extend, getting the fly ready to eat. The PER is a consistent and strong reaction to appealing tastes and is used to measure the fly's feeding behaviour.[22]

Dopamine acts as a strong reinforcer for both positive and negative associative memories .[23] *Drosophila*'s aversive taste memory is an excellent model for exploring how the brain changes behavior and processes sensory information. Sweet and bitter taste neurons control automatic acceptance or rejection behaviors, and changes in these natural responses depend on the MBs. [24]

2.6. LEAKY INTEGRATE AND FIRE MODEL :

The nerve cell membrane acts as a barrier between the intracellular and extracellular fluids, maintaining a more negative charge inside the cell compared to the outside when in a resting state. The cell membrane's electrical properties can be represented by a parallel circuit comprising membrane capacitance (C), and membrane resistance (R), in series with a battery having an electromotive force (emf) equivalent to the resting potential (V_{rest}), influenced by an external stimulus. (Matlab Physics).

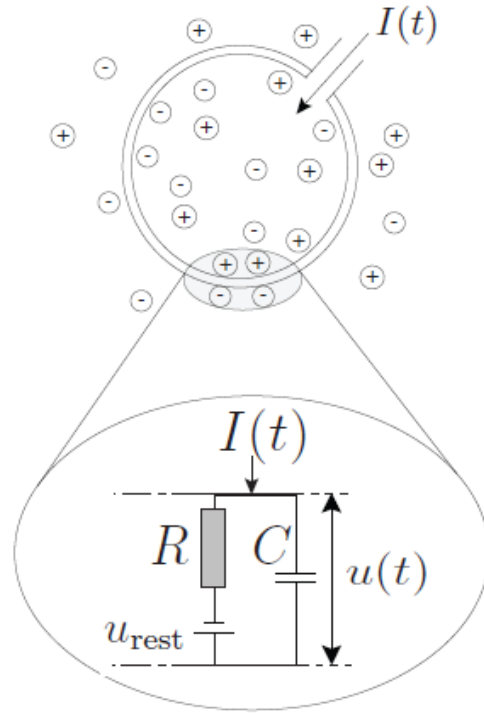


Figure 5: circuit representation of biological neuron (Gerstner et al., 2014)

The variable v_i represents the membrane potential of neuron i at any given moment. When there is no external input, the potential stays at its resting value, v_{rest} . However, if an experimenter applies a current $I(t)$ to the neuron or it receives synaptic input from other neurons, the potential v_i changes from its resting state [25].

To derive an equation connecting the momentary voltage $v_i(t) - v_{rest}$ to the input current $I(t)$, fundamental principles from the field of electricity are employed. A neuron is encompassed by a cellular membrane, which exhibits high insulating properties. Upon introduction of a brief current pulse $I(t)$ into the neuron, the excess electric charge ($q = \int I(t') dt'$) needs to be accommodated, typically leading to the charging of the cell membrane. Consequently, the cell membrane behaves like a capacitor with a specific

capacitance C . Due to the imperfect nature of the insulator, the charge gradually dissipates across the cell membrane with time. Thus, the cell membrane can be defined by a finite leakage resistance (R) . [25]

The fundamental electrical circuit of a leaky integrate-and-fire model comprises a capacitor (C) , in parallel with a resistor (R) , driven by a current $I(t)$

The leaky integrate-and-fire (LIF) model is a simple way to understand how neurons work. It has two main parts: the integrative part and the leaky part. These parts together control how the neuron's membrane potential changes over time [26].

In the integrate component of the model, the neuron accumulates incoming electrical signals over time. These inputs can be synaptic inputs from other neurons or externally applied currents. The impact of these inputs on the membrane potential v_t is described by:

$$C \frac{dv}{dt} = I(t)$$

where:

- C is the membrane capacitance,
- dv/dt is the rate of change of the membrane potential,
- $I(t)$ = the input current at time t .

This equation indicates that the rate of change of the membrane potential is proportional to the input current. As the neuron receives more input currents, the membrane potential increases over time.

The leaky component of the model reflects the fact that the neuron's membrane is not a perfect insulator. Over time, the membrane potential tends to decay back towards a resting potential V_{rest} due to the leakage of charge through the

membrane. This leakage can be modelled as a resistor R in parallel with the capacitor C . The corresponding term in the differential equation is:

$$-\frac{v_t - v_{rest}}{R}$$

where:

- v_t is the membrane potential at time t ,
- V_{rest} is the resting potential,
- R is the membrane resistance.

This term describes the decay of the membrane potential towards the resting potential, with the rate of decay determined by the membrane resistance.

Combining the integrate and leaky components, the complete differential equation for the LIF model is:

$$I(t) = \frac{v(t) - v_{rest}}{R} + C \frac{dv}{dt}$$

using the membrane time constant $\tau_m = RC$

$$\tau_m \frac{dv}{dt} = -[v(t) - v_{rest}] + RI(t)$$

In addition to the integrate and leaky components, the LIF model includes a firing mechanism.

When the membrane potential v_t hits a certain threshold v_{th} , the neuron sends out a spike (an action potential). After this happens, the membrane potential drops back to a reset level v_{reset} , and the neuron might go through a short time where it can't fire again, called the refractory period [25].

Alpha synapse dynamics describe how synaptic currents evolve over time in response to a presynaptic action potential. Characterized by a rapid rise to a peak value followed by an exponential decay, the dynamics of synaptic conductance are captured by the differential equation:

$$dg/dt = -g/Tau$$

Here, tau represents the synaptic decay time constant, indicating the exponential decrease of conductance (g) following a sudden increase caused by a presynaptic spike. Consequently, after the initial perturbation in membrane potential, g gradually diminishes until reaching 0, leading the membrane potential back to its resting state. Upon neuronal firing, the membrane potential is restored to its baseline and remains stable throughout the refractory period.

The membrane potential is described by:

$$dv/dt = (g - (v - V_{resting}))/T_{mbr}$$

$V_{resting}$ is the resting membrane potential, and T_{mbr} is the membrane time constant. This time constant is calculated by multiplying the membrane resistance R_{mbr} by the membrane capacitance C_{mbr} [27, 28, 29, 30]

We simulated the impact of sugar neuron spiking on dopaminergic neurons activity using a computational method, a LIF [31] based on neuronal connection and neurotransmitter identity. We hope to understand more about how sugar neurons as well as aversive neurons spiking effects dopaminergic neuron activity and its possible consequences for reward processing and decision-making in the drosophila brain.

Developing brain circuit models based on connectivity and predicted neurotransmitter types lead to development of hypotheses which can be tested experimentally. Each neuron has several downstream neurons and it becomes

difficult to draw functional connectivity while studying behaviours . The method used by Shiu et al., 2023 takes connection weights from the fruit fly connectome. When a neuron spikes, it changes the membrane potential of connected downstream neurons according to the strength of their connections. If the downstream neuron's membrane potential goes beyond the firing threshold, it fires. We used the spiking neural network simulator Brian2 to build this model. Each neuron starts with a firing rate of 0 Hz. By activating a few neurons, we can predict how this will change the firing rates of connected neurons [31].

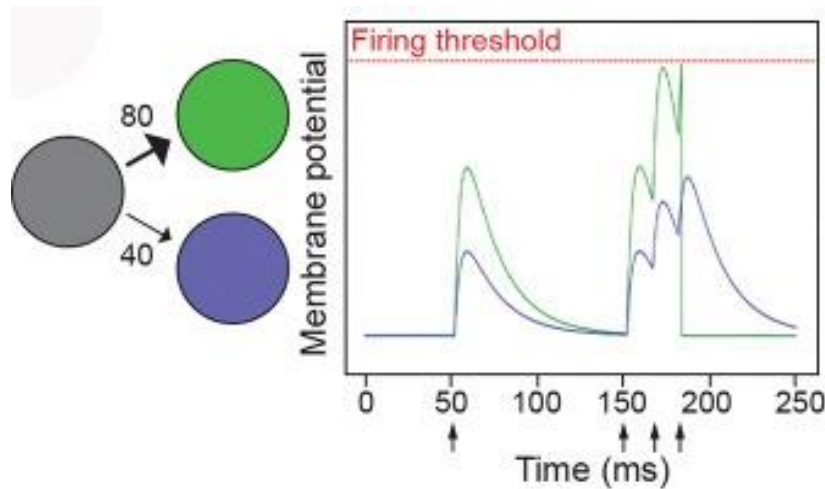


Figure 6 : Diagram of the LIF. 80, 40 represents the connectivity proportion [31].

2.7. OBJECTIVES:

- Simulate the effects of spiking sugar neurons on dopaminergic neuron activity: To simulate the impact of spiking sugar neurons on the firing patterns and activity of dopaminergic neurons using the leaky integrate-and-fire model.
- To specifically simulate subset of dopaminergic neurons PAM and PPL that are involved in sugar sensing and aversive sensing respectively and see the effects.
- Analyse the sugar neuron modulation on dopaminergic neurons: To assess the functional implications of sugar neuron modulation on dopaminergic neuron activity. Compare the activity of DANs before and after spiking sugar neurons. Identify significant changes in firing rates or patterns in DANs induced by sugar neuron activity.

3. METHODOLOGY:

Implemented LIF model incorporating α -synapse dynamics, following the methodologies outlined by [31, 32, 33, 34]. This model simulates the impact of synaptic inputs on neuronal firing patterns using the following differential equations and parameters:

$$dv/dt = (g - (v - V_{resting}))/T_{mbr}$$

$$dg/dt = -g/Tau$$

Parameters

- Resting potential ($V_{resting}$): -52 mV (Kakaria and de Bivort, 2017)
- Reset potential after spike (V_{reset}): -52 mV (Kakaria and de Bivort, 2017)
- Threshold for spiking ($V_{threshold}$): -45 mV (Kakaria and de Bivort, 2017)
- Membrane resistance (R_{mbr}): 10 M Ω (Kakaria and de Bivort, 2017)
- Refractory period ($T_{refractory}$): 2.2 ms (Kakaria and de Bivort, 2017; Lazar et al., 2021)
- Membrane capacitance (C_{mbr}): 0.002 μ F (Kakaria and de Bivort, 2017)
- Membrane time scale (T_{mbr}): Calculated as $T_{mbr} = C_{mbr} * R_{mbr}$
- Synapse decay time scale (τ): 5 ms (Jürgensen et al., 2021)
- Time delay from spike to change in membrane potential (T_{dly}): 1.8 ms (Paul et al., 2015)
- Synaptic weight (W_{syn}): 0.275 mV, a parameter representing the synapse's influence on the downstream membrane potential.

In the present framework, the membrane potential (v) of the neuron reverts to its resting potential ($V_{resting}$) in the absence of stimulation. Upon activation of an upstream neuron, alterations in the membrane potential occur based on

the synaptic connections. Activation of an excitatory upstream neuron results in depolarization of the neuron, whereas activation of an inhibitory neuron leads to hyperpolarization.

All parameters in this model are based on previous *Drosophila* research and electrophysiological data from studies. Synaptic weights were obtained from the Flywire connectome by [35,36] along with neurotransmitter predictions from [6]. The only variable parameter, W_{Syn} , reflects the change in the membrane potential of downstream neurons due to a single excitatory or inhibitory synapse. This parameter was adjusted so that when sugar-sensitive GRNs are activated at 100 Hz, it results in about 80% of the maximum firing rate of MN9 motor neurons, as reported by [31].

The strength of the synaptic connection between two neurons, denoted as weight (w), is influenced by the synaptic connectivity weight derived from the Flywire connectivity. This weight is adjusted by a factor of 1 for excitatory upstream neurons and -1 for inhibitory ones, then further altered by W_{syn} . When the upstream neuron fires, the neuron-specific parameter g is modified to $g + w$. Initially, or when the neuron fires, g is initialized to 0 mV.[31]

1.Data Preparation:

- Load the connectivity file representing synaptic connections between neurons in the *Drosophila* brain. Taken from https://github.com/philshiu/Drosophila_brain_model/blob/main/2023_03_23_connectivity_630_final.parquet
- Querying database : Extract the neuron IDs for sugar neurons and DANs from Flywire dataase.[40]

2.Simulation: Run computational simulations using brian2 [39] simulator to observe the spiking of sugar neurons at different frequencies (25 Hz, 50 Hz, 75

Hz, 100 Hz, 125 Hz, 150Hz, 175Hz, 200Hz) affecting the firing rates and patterns of dopaminergic neurons using the leaky integrate-and-fire model.

3.Data Collection and Analysis: Analyse the changes in firing rates of dopaminergic neurons in response to spiking sugar neurons. Use Matplotlib and Seaborn to plot highlighting the interaction between sugar neurons and DANs.

4. RESULTS:

4.1. SPIKING PPL1- γ 1pedc FROM 0 to 200 Hz:

- Stimulating PPL1- γ 1pedc neurons promotes strong aversive odour memory formation.(Aso et al.,2014)

| root_id | label | cell_type | side |
|--------------------|---|------------|-------|
| 720575940617691170 | ['PPL101; γ 1ped; FBbt_00100243'; 'PPL101; γ 1ped'] | ['PPL101'] | right |
| 720575940621040737 | ['PPL101; γ 1ped; FBbt_00100243'; 'PPL101; γ 1ped'] | ['PPL101'] | left |

Table 1 : Root-ids of set of PPL1- γ 1pedc activated.

- PPL1- γ 1pedc; a dopaminergic neuron from the PPL1 cluster terminals overlap with the dendrites of MBON- γ 1pedc α/β , short name – MBON-11 (Aso et al., 2014)
- Activation of just PPL1- γ 1pedc activates a list of KCs and MBONS. Two of the MBONs show more activity which belong MBON11. Their Flywire ids are, root_id=720575940617749538, 720575940623201833 .

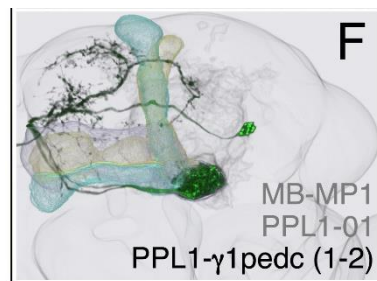


Figure 7: PPL1- γ 1pedc; a DAN of the PPL1 cluster with terminals that overlap with the dendrites of MBON- γ 1pedc α/β . (Aso et al., 2014)

| ROOT ID | CLASS | HEMIBRAIN_TYPE |
|--------------------|-------|----------------|
| 720575940617749538 | MBON | MBON11 |
| 720575940623201833 | MBON | MBON11 |

Table 2 : Root-ids of set of MBON11 that was activated after activation of PPL1-γ1pedc showing connectivity between them.

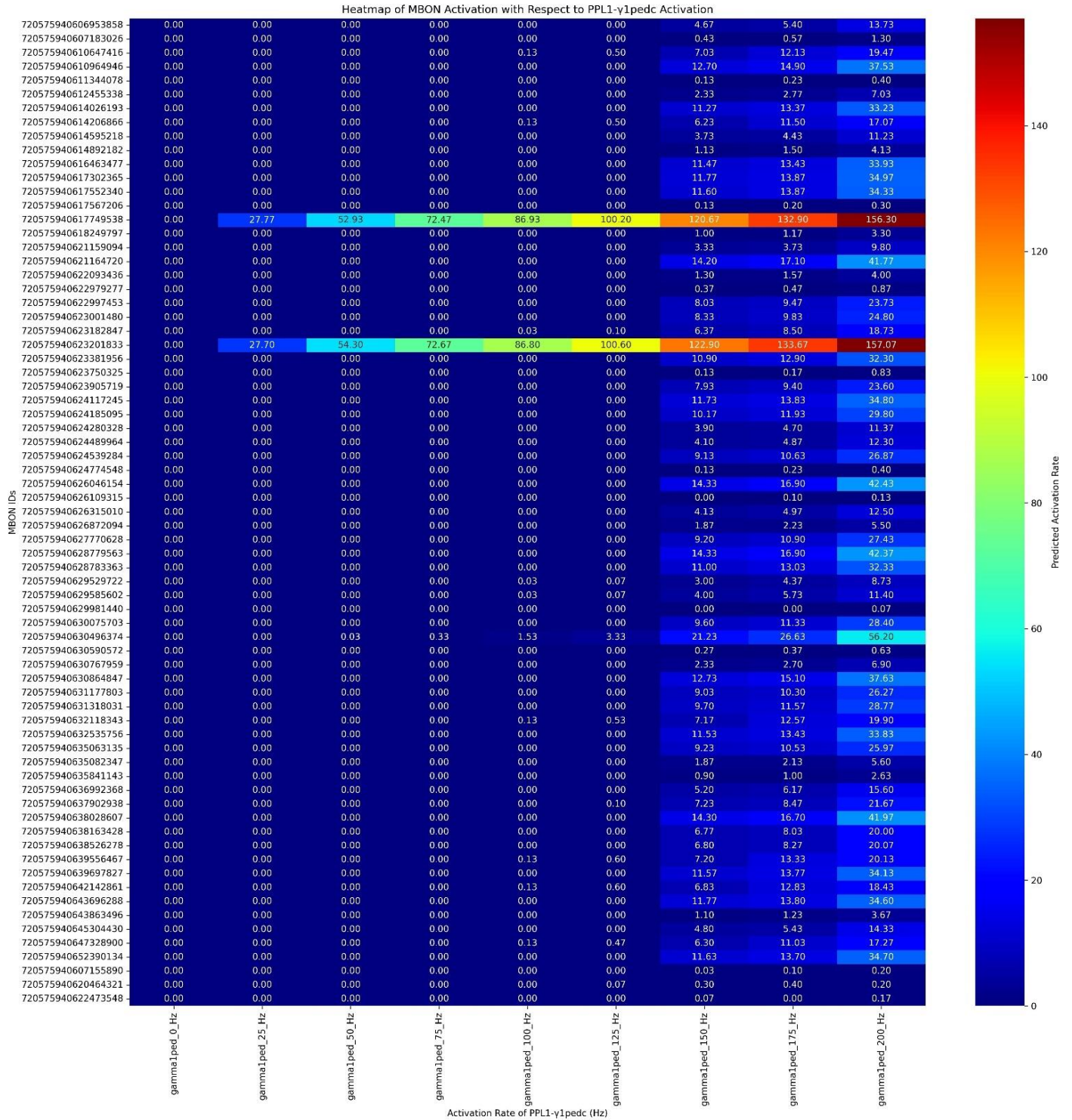


Figure 8 : Heatmap shows the firing rates of MBONs in responding to 0 to 200 Hz PPL1-γ1pedc firing. The y-axis depicts the MBON IDs

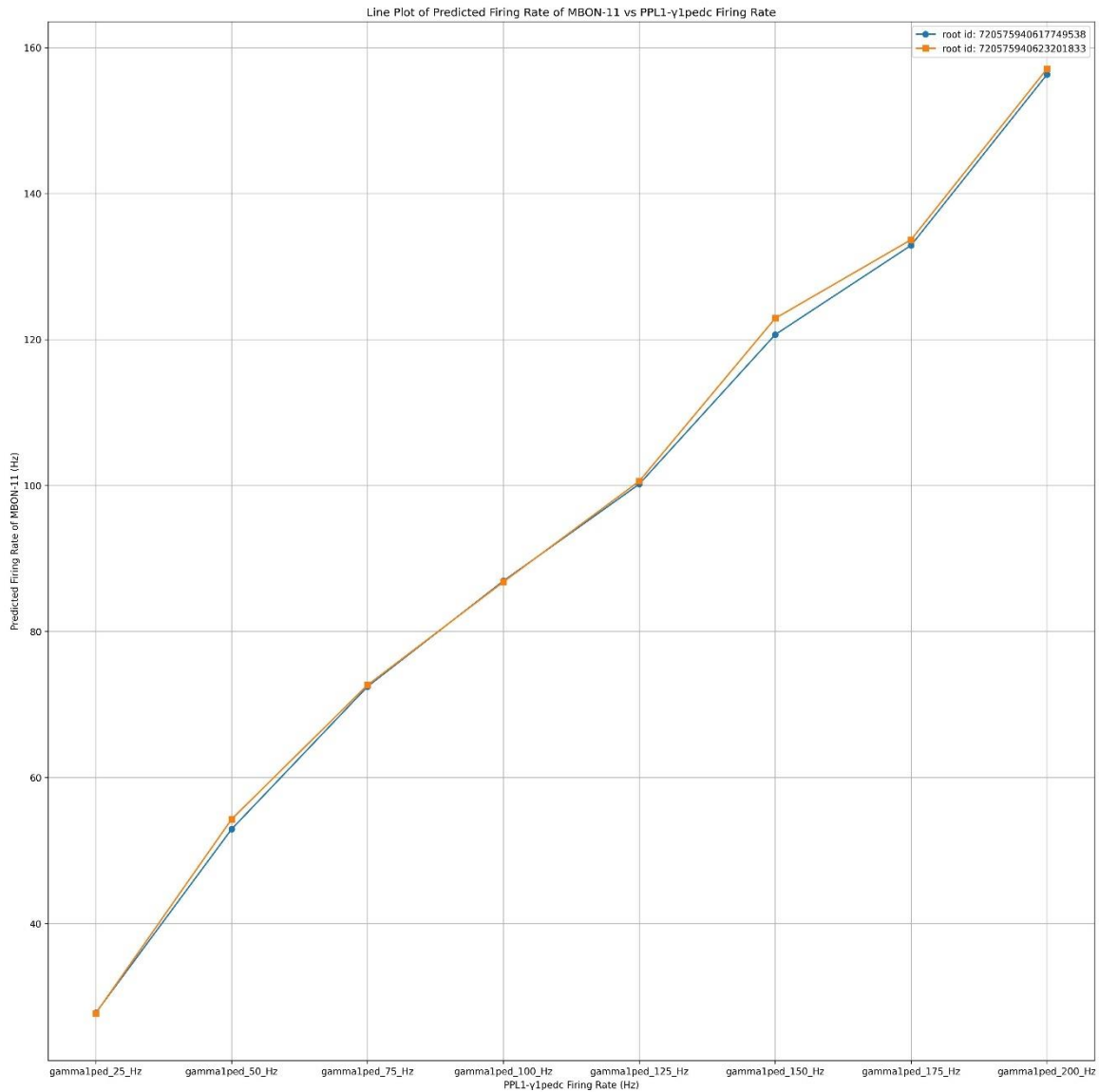


Figure 9 : Lineplot depicting the predicted firing rate of two MBON11 ids
X axis- depicts the PPL1-γ1pedc firing rate from 0 to 200 Hz and y axis depicts the predicted firing rate of PPL1-γ1pedc.

4.2. SPIKING PAM- β '2a FROM 0 to 200 Hz:

- Activation of PAM- β '2a activates MBON1 and MBON3 which are neurons that are post-synaptic to PAM- β '2 (Scaplen et al.,2020; Aso et al., 2014)
- The activation of MBONs by PAM- β '2 tells us the model is working.

| root_id | label | cell_type | side |
|--------------------|---------------------------------|-----------------------|-------|
| 720575940640048768 | ['PAM02; B`2a'] | ['PAM02'] | left |
| 720575940630998287 | ['PAM02; B`2a'; 'fru'; 'PAM01'] | ['PAM02'; 'PAM01'] | left |
| 720575940631118610 | ['PAM02; B`2a'; 'fru'; 'PAM01'] | ['PAM02'; 'PAM01'] | left |
| 720575940628708139 | ['PAM02; B`2a'] | ['PAM02'] | right |
| 720575940613732271 | ['PAM02; B`2a'] | ['PAM02'] | left |
| 720575940620497217 | ['PAM02; B`2a'] | ['PAM02'] | right |
| 720575940630794703 | ['PAM02; B`2a'; 'fru'; 'PAM01'] | ['PAM01'] | right |
| 720575940630816207 | ['PAM02; B`2a'; 'fru'; 'PAM01'] | ['PAM01'] | left |
| 720575940632541523 | ['PAM01; y5'; 'PAM02; B`2a'] | ['PAM02'] | left |
| 720575940636355685 | ['PAM02; B`2a'] | ['PAM02'] | left |
| 720575940635779959 | ['PAM02; B`2a'] | ['PAM02'] | right |
| 720575940630498811 | ['PAM02; B`2a'; 'fru'; 'PAM01'] | ['PAM01'] | right |

Table 3 : Root-ids of set of PAM- β '2a activated.

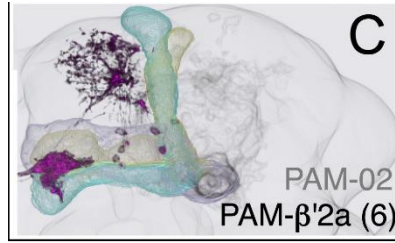


Figure : PAM- β' 2a neurons.

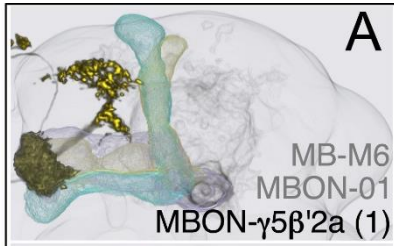


Figure : MBON1 neurons.

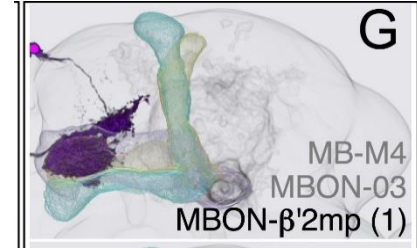


Figure : MBON3 neurons.

Figure 10: Figures representing PAM- β' 2a neurons, MBO-01 and MBON-03 neurons. (Aso et al., 2014)

| Root_id | class | Hemibrain_type | side | Cell type |
|--------------------|-------|----------------|-------|--------------------------|
| 720575940624117245 | MBON | MBON01 | right | MBON- $\gamma 5\beta'2a$ |
| 720575940624694503 | MBON | MBON03 | left | MBON- $\beta'2mp$ |

Table 4: Root-ids of a set of MBONs that were activated after activation of PAM- β' 2a showing connectivity between them.

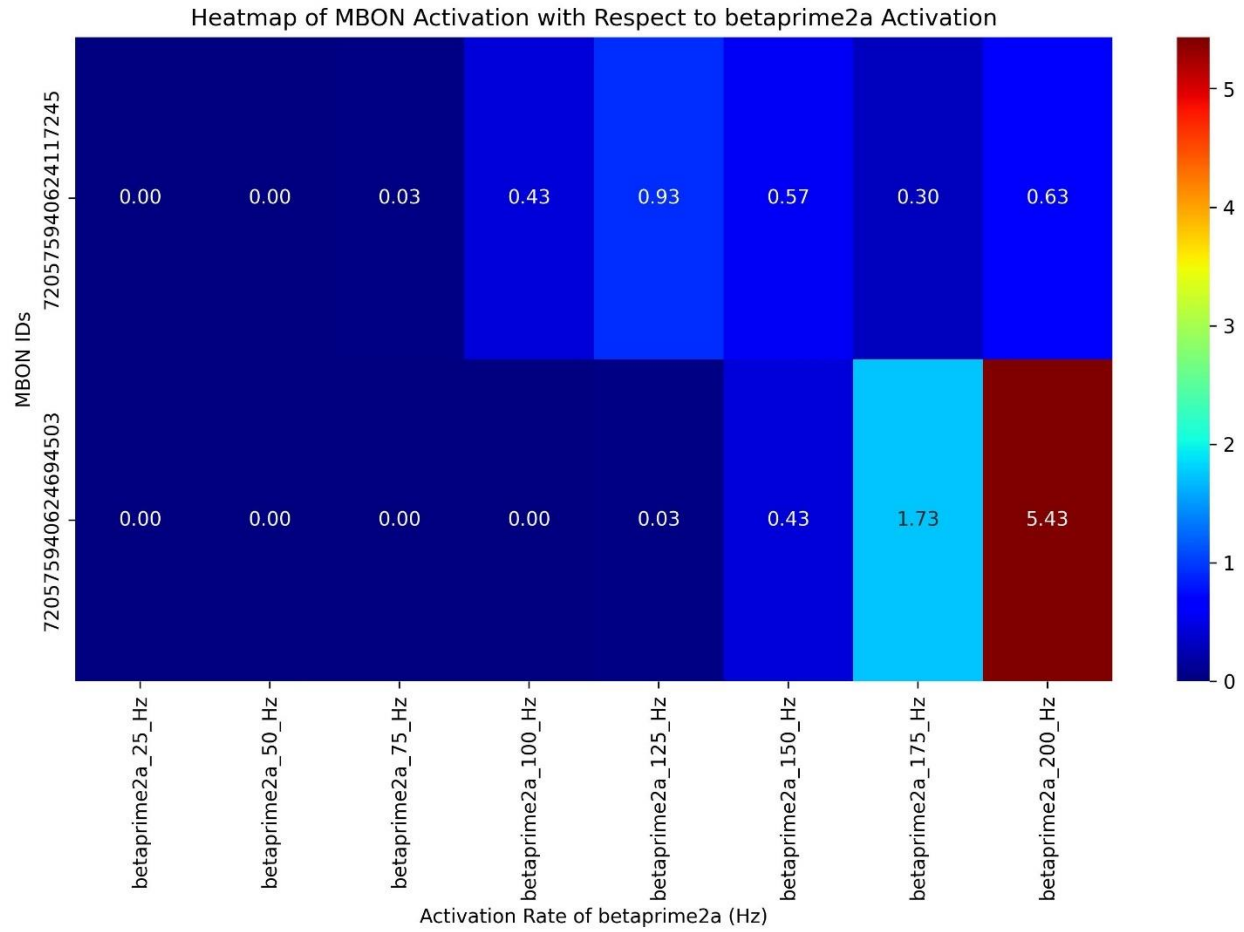


Figure 11: Heatmap showing firing rates of MBONs in response to activation of PAM- β' 2a unilateral 0 to 200 Hz . The y-axis depicts the MBON IDs , and x-axis depicts the activation of PAM- β' 2a from 0 to 200 Hz.

4.3. SPIKING SUGAR NEURONS:

- When a set of sugar neurons was simulated to study the effect on dopaminergic neurons, it didn't activate DANDS or any of the neurons involved in sugar and reward system circuitry as shown in figure 14 but a set of descending neurons (DNs), motor neurons as well as MBON35.

Virtual fly brain (VFB): Sugar neuron visualized in virtual fly brain 3-D viewer to understand the circuitry better. <https://www.virtualflybrain.org/>

- sugar-sensing neuron of labellar taste bristle GRN R4#16 (FAFB:14928124) [VFB_00102914] was visualised in VFB.

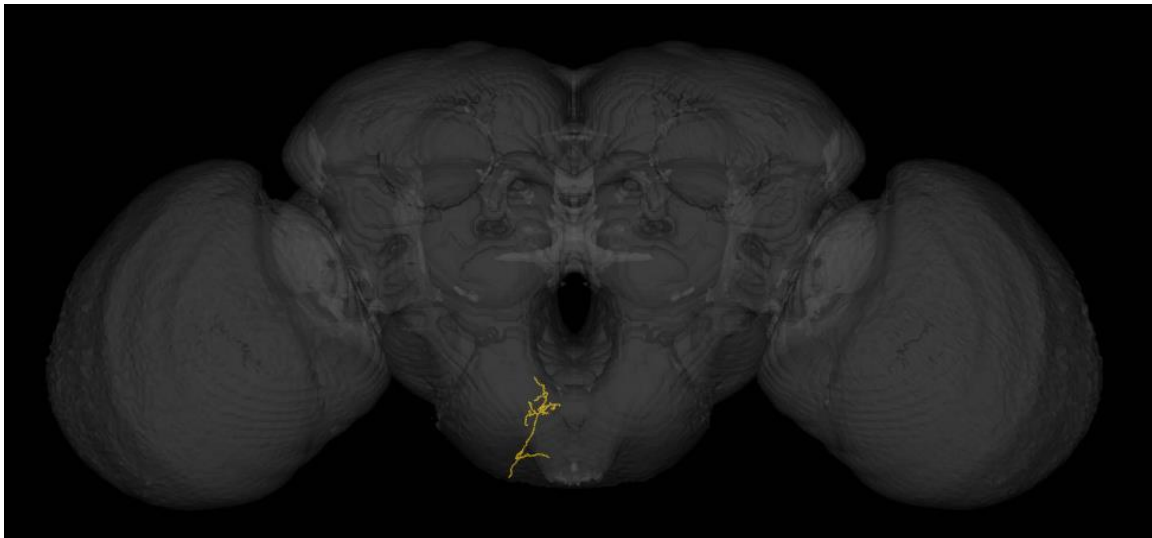


Figure 12: GRN R4#16 (FAFB:14928124) [VFB_00102914] visualized in VFB.

- Putative DAN PAM-B'2a (4) 1683766 was visualised in VFB

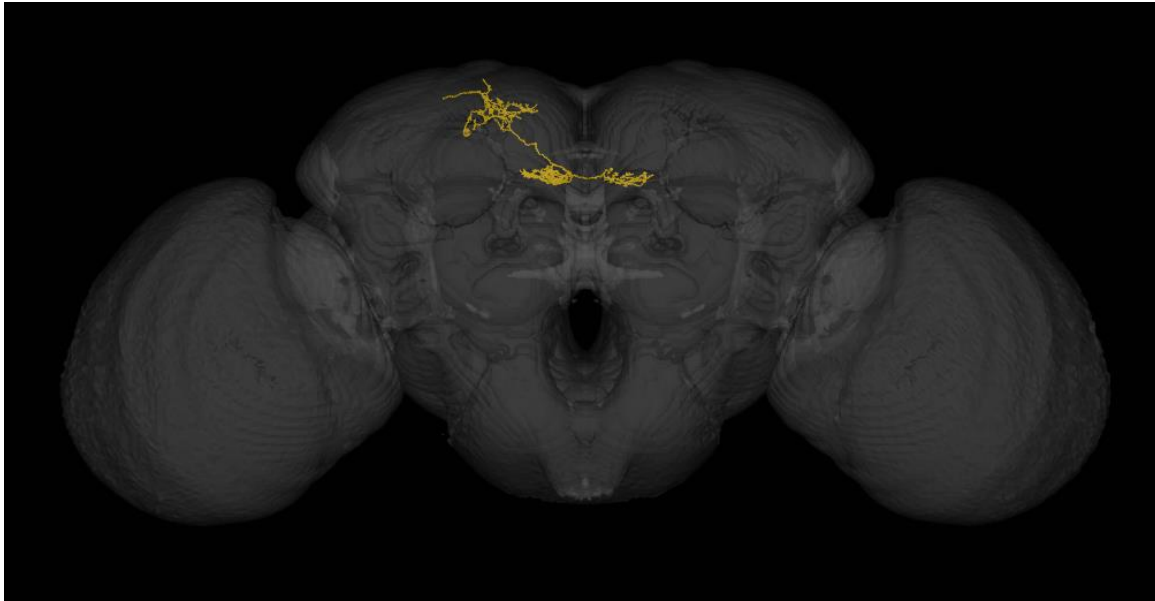


Figure 13 : PAM-b'2(c1)#1_R (FAFB:8317886) [VFB_00101418] Visualised in VFB

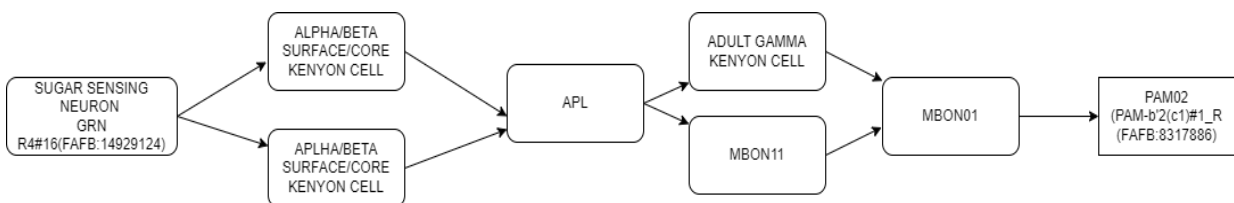


Figure 14: The reconstructed circuitry between sugar sensing gustatory neuron and PAMB`2 using VFB circuit browser.

<https://www.virtualflybrain.org/> reconstructed via

<https://app.diagrams.net/>

| root_id | class | side |
|--------------------|-----------|-------|
| 720575940639332736 | gustatory | left |
| 720575940617000768 | gustatory | left |
| 720575940630094652 | | right |
| 720575940637568838 | gustatory | left |
| 720575940624963786 | gustatory | left |
| 720575940622474899 | | right |
| 720575940629176663 | gustatory | left |
| 720575940633143833 | gustatory | left |
| 720575940640649691 | gustatory | left |
| 720575940620900446 | gustatory | left |
| 720575940613601698 | gustatory | left |
| 720575940616885538 | gustatory | left |
| 720575940621502051 | gustatory | left |
| 720575940610788069 | gustatory | left |
| 720575940628676457 | | left |
| 720575940612670570 | gustatory | left |
| 720575940623172843 | gustatory | left |
| 720575940638202345 | gustatory | left |
| 720575940632889389 | gustatory | left |
| 720575940636895406 | | left |
| 720575940611875570 | gustatory | left |
| 720575940612289010 | | left |
| 720575940628853239 | gustatory | left |
| 720575940635239672 | | right |
| 720575940630797113 | gustatory | left |
| 720575940621754367 | gustatory | left |
| 720575940630233916 | gustatory | left |
| 720575940639198653 | gustatory | left |
| 720575940632425919 | gustatory | left |

TABLE 5 : Root-ids of sugar neurons that were activated.

The gustatory system must transmit information from sugar receptors to motor neurons in the VNC to drive behaviours such as approach or avoidance in response to sugar. This complex pathway involves several key neural structures, including the MBONs and DNs. The connection is facilitated by

several hundred descending neurons (DNs) that traverse the neck to reach motor neuropils in the VNC [37] . Although direct synaptic connections between MBONs and DNs have not been conclusively documented, MBON35 is believed to connect to neurons that likely include DNs. This potential connection warrants further anatomical verification but suggests a plausible pathway for information flow.

MBON35 projects to regions such as the lateral accessory lobe (LAL). While the direct synaptic link between MBON35 and DNs has not been explicitly demonstrated, MBON35's projections to the LAL suggest it could influence DNs indirectly through intermediate neurons or shared neuropil regions. This indirect pathway is a critical area for further exploration, as it may elucidate how sensory information processed by the MB can translate into motor commands. [11,35]

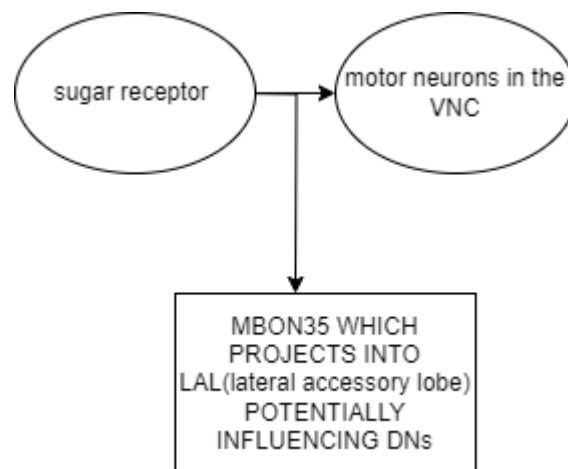


Figure 15 : Simplified pathway depiction between sugar gustatory and motor system [11,35]

4.4. SPIKING SUGAR AS WELL AS DOPAMINERGIC NEURONS FROM 0 to 200 Hz:

When both a set of sugar neurons and dopaminergic neurons were activated to study their combined effect on dopaminergic neurons, the expectation was that sugar activation would suppress the activity of already active aversive PPL1-y1pedc neurons. However, the results showed that sugar activation did not have any enhancing or suppressive effects on either of the dopaminergic neurons studied.

Refer to table no 5 for list of sugar ids activated and table no 1 for list of PPL1-y1pedc neurons activated.

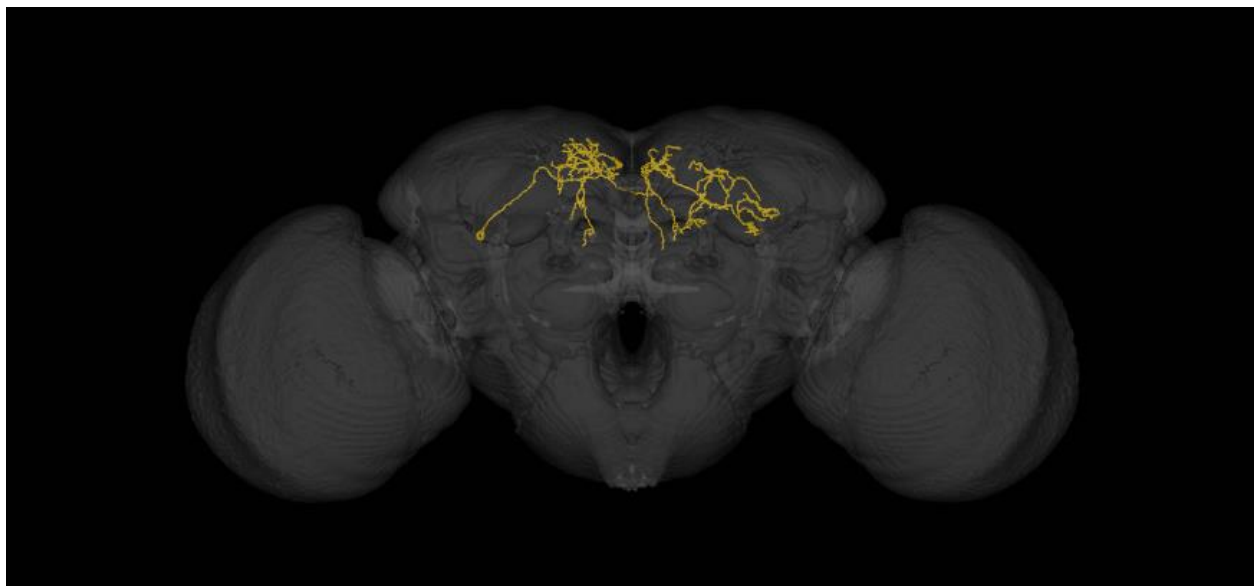


Figure 16 : PPL1-y1_R (FAFB:6893931) [VFB_001014ie]

DAN PPL1-y1 Right 6893932 JS MWP visualised in VFB

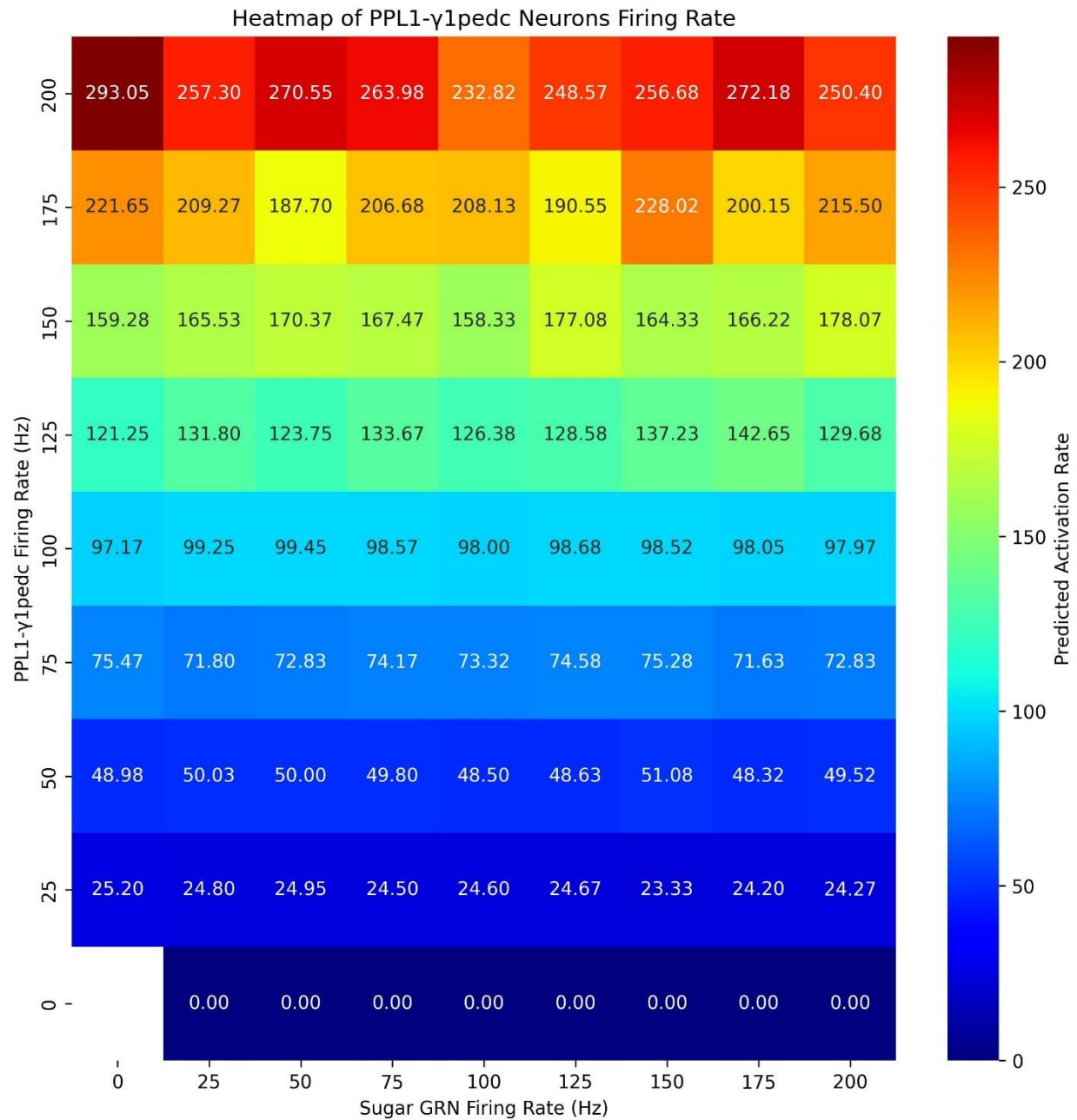


Figure 17 : The heatmap displays the predicted activation rate (color scale on the right) as a function of two variables: the firing rate of PPL1-γ1pedc neurons (y-axis) ranging from 0 to 200 Hz and the firing rate of Sugar GRN (gustatory receptor neurons) (x-axis) ranging from 0 to 200 Hz.

- When sugar activity is at 0 Hz, the PPL1-γ1pedc activated at 200 Hz gives a predicted firing rate of 293.05.
- At 200 Hz, when both sugar and PPL1-γ1pedc neurons are activated the activity of PPL1-γ1pedc neurons drops from 293.05 to 250.40 indicating there is some suppression of activity of PPL1-γ1pedc neurons due to sugar activation.

5. DISCUSSION AND CONCLUSION :

- Spiking PPL1- γ 1pedc from 0 to 200 Hz: The stimulation of PPL1- γ 1pedc neurons from 0 to 200 Hz significantly promotes aversive memory formation, corroborating the findings of Aso et al. (2014). This was demonstrated by the activation of a specific set of KCs and MBONs, particularly MBON- γ 1pedc α/β , also known as MBON-11. The heatmap and line plot depicting the firing rates of MBONs in response to PPL1- γ 1pedc firing further confirm the connectivity and functional impact of these neurons. This indicates the model's functionality in replicating known synaptic connections.
- Spiking PAM- β '2a from 0 to 200 Hz: Activation of PAM- β '2a neurons from 0 to 200 Hz successfully activated MBON1 and MBON3, which are post-synaptic to PAM- β '2a neurons. This result aligns with previous studies by [38] , indicating the model works by simulating neuronal activity and its downstream effects. The heatmap provided evidence even though the activity was sparse.
- Spiking Sugar Neurons: When simulating the spiking of a set of sugar neurons, the expected activation of dopaminergic neurons (DANs) and other neurons involved in the sugar-reward circuitry was not observed. Instead, the activation led to the firing of descending neurons (DNs) and motor neurons, as well as MBON35. This unexpected result suggests a complex pathway where sugar information is relayed from gustatory neurons to motor neurons via intermediate structures, possibly including the MBONs and DNs, as suggested by [37,11] , highlighting the complexity of the gustatory system's influence on behaviour.
- The lack of observed effects of sugar neuron activation on DANs suggests that direct modulatory effects may be limited or influenced by unaccounted factors in the current model.
- Spiking Sugar and Dopaminergic Neurons from 0 to 200 Hz: When both sugar neurons and dopaminergic neurons were activated simultaneously,

it was hypothesized that sugar activation would suppress the activity of the aversive PPL1- γ 1pedc neurons. The results partially supported this hypothesis, showing a reduction in the predicted firing rate of PPL1- γ 1pedc neurons from 293.05 to 250.40 when both neuron types were activated at 200 Hz. This indicates a moderate suppression effect of sugar neuron activation on PPL1- γ 1pedc neurons, suggesting potential interactions between the sugar and aversive memory systems.

- Simultaneous activation of both sugar neurons and dopaminergic neurons to observe any potential modulatory effects revealed that sugar neuron activation sparsely suppressed, there is no significant suppression in the activity of the DANs studied.
- These findings suggest that the direct modulatory effects of sugar neuron activation on the DANs might be limited or influenced by additional factors not accounted for in the current model. Further investigation is needed to explore the underlying mechanisms and interactions between sugar neurons and dopaminergic circuits.

6. FUTURE WORK :

- To improve the model's accuracy, we can explore varying the synaptic weights between sugar neurons, DANs, and MBONs.
- Analyse the topological properties of the *Drosophila* connectome, and connectivity, to reveal critical nodes and pathways that influence the overall network. Altering network topology parameters can help simulate different brain states and their behavioural outcomes.
- KCs, MBONs, and DANs form an extensive network of feedback loops that play a critical role in learning and memory in the *Drosophila* brain. Incorporating these feedback loops into computational models can significantly enhance our understanding of the dynamic processes underlying neural plasticity and behaviour. Feedback loops often involve multiple, intersecting pathways, making it difficult to isolate the contribution of individual connections.
- Once we change the parameters and weights, this model can be standardized to study other taste modalities like fat sensation.

7. REFERENCES:

- [1] May, C. E., Rosander, J., Gottfried, J., Dennis, E., & Dus, M. (2020). Dietary sugar inhibits satiation by decreasing the central processing of sweet taste. *Elife*, 9, e54530.
- [2] Dvořáček, J., & Kodrik, D. (2021). *Drosophila* reward system-A summary of current knowledge. *Neuroscience & Biobehavioral Reviews*, 123, 301-319.
- [3] Aso, Y., Hattori, D., Yu, Y., Johnston, R. M., Iyer, N. A., Ngo, T. T., ... & Rubin, G. M. (2014). The neuronal architecture of the mushroom body provides a logic for associative learning. *elife*, 3, e04577.
- [4] Schlegel, P., Yin, Y., Bates, A. S., Dorkenwald, S., Eichler, K., Brooks, P., ... & Jefferis, G. S. X. E. (2023). A consensus cell type atlas from multiple connectomes reveals principles of circuit stereotypy and variation. *Biorxiv: the Preprint Server for Biology*.
- [5] Dorkenwald, S., Matsliah, A., Sterling, A. R., Schlegel, P., Yu, S. C., McKellar, C. E., ... & FlyWire Consortium. (2023). Neuronal wiring diagram of an adult brain. *bioRxiv*.
- [6] Eckstein, N., Bates, A. S., Champion, A., Du, M., Yin, Y., Schlegel, P., ... & Funke, J. (2024). Neurotransmitter classification from electron microscopy images at synaptic sites in *Drosophila melanogaster*. *Cell*, 187(10), 2574-2594.
- [7] Liu, W. W., & Wilson, R. I. (2013). Glutamate is an inhibitory neurotransmitter in the *Drosophila* olfactory system. *Proceedings of the National Academy of Sciences*, 110(25), 10294-10299.
- [8] McCarthy, E. V., Wu, Y., Decarvalho, T., Brandt, C., Cao, G., & Nitabach, M. N. (2011). Synchronized bilateral synaptic inputs to *Drosophila melanogaster* neuropeptidergic rest/arousal neurons. *Journal of Neuroscience*, 31(22), 8181-8193.
- [9] Molina-Obando, S., Vargas-Fique, J. F., Henning, M., Gür, B., Schladt, T. M., Akhtar, J., ... & Silies, M. (2019). ON selectivity in the *Drosophila* visual system is a multisynaptic process involving both glutamatergic and GABAergic inhibition. *Elife*, 8, e49373.
- [10] Tanaka, N. K., Tanimoto, H., & Ito, K. (2008). Neuronal assemblies of the *Drosophila* mushroom body. *Journal of Comparative Neurology*, 508(5), 711-755.

- [11] Li, F., Lindsey, J. W., Marin, E. C., Otto, N., Dreher, M., Dempsey, G., ... & Rubin, G. M. (2020). The connectome of the adult *Drosophila* mushroom body provides insights into function. *Elife*, 9, e62576.
- [12] Claridge-Chang, A., Roorda, R. D., Vrontou, E., Sjulson, L., Li, H., Hirsh, J., & Miesenböck, G. (2009). Writing memories with light-addressable reinforcement circuitry. *Cell*, 139(2), 405-415.
- [13] Galili, D. S., Dylla, K. V., Lüdke, A., Friedrich, A. B., Yamagata, N., Wong, J. Y. H., ... & Tanimoto, H. (2014). Converging circuits mediate temperature and shock aversive olfactory conditioning in *Drosophila*. *Current biology*, 24(15), 1712-1722.
- [14] Masek, P., Worden, K., Aso, Y., Rubin, G. M., & Keene, A. C. (2015). A dopamine-modulated neural circuit regulating aversive taste memory in *Drosophila*. *Current biology*, 25(11), 1535-1541.
- [15] Burke, C. J., Huetteroth, W., Oswald, D., Perisse, E., Krashes, M. J., Das, G., ... & Waddell, S. (2012). Layered reward signalling through octopamine and dopamine in *Drosophila*. *Nature*, 492(7429), 433-437.
- [16] Liu, C., Plaçais, P. Y., Yamagata, N., Pfeiffer, B. D., Aso, Y., Friedrich, A. B., ... & Tanimoto, H. (2012). A subset of dopamine neurons signals reward for odour memory in *Drosophila*. *Nature*, 488(7412), 512-516.
- [17] Mao, Z., & Davis, R. L. (2009). Eight different types of dopaminergic neurons innervate the *Drosophila* mushroom body neuropil: anatomical and physiological heterogeneity. *Frontiers in neural circuits*, 3, 612.
- [18] Tomchik, S. M. (2013). Dopaminergic neurons encode a distributed, asymmetric representation of temperature in *Drosophila*. *Journal of Neuroscience*, 33(5), 2166-2176.
- [19] Das, G., Klappenbach, M., Vrontou, E., Perisse, E., Clark, C. M., Burke, C. J., & Waddell, S. (2014). *Drosophila* learn opposing components of a compound food stimulus. *Current biology*, 24(15), 1723-1730.
- [20] Lin, S. (2023). The making of the *Drosophila* mushroom body. *Frontiers in Physiology*, 14, 1091248.
- [21] Cognigni, P., Felsenberg, J., & Waddell, S. (2018). Do the right thing: neural network mechanisms of memory formation, expression and update in *Drosophila*. *Current opinion in neurobiology*, 49, 51-58.

- [22] Masek, P., & Keene, A. C. (2016). Gustatory processing and taste memory in *Drosophila*. *Journal of neurogenetics*, 30(2), 112-121.
- [23] Waddell, S. (2010). Dopamine reveals neural circuit mechanisms of fly memory. *Trends in neurosciences*, 33(10), 457-464.
- [24] Aso, Y., Siwanowicz, I., Bräcker, L., Ito, K., Kitamoto, T., & Tanimoto, H. (2010). Specific dopaminergic neurons for the formation of labile aversive memory. *Current biology*, 20(16), 1445-1451.
- [25] Gerstner, W. 1.3 Integrate-And-Fire Models | Neuronal Dynamics online book. Copyright © Cambridge University Press 2014. Available at: <https://neurondynamics.epfl.ch/online/Ch1.S3.html>.
- [26] Schmitt, O., Eipert, P., Wang, Y., Kanoke, A., Rabiller, G., & Liu, J. (2023). Connectome-based prediction of functional impairment in experimental stroke models. *bioRxiv*.
- [27] Dayan, P., and Abbott, L. F. 2001. *Theoretical Neuroscience: Computational and Mathematical Modeling of Neural Systems*. Available at: <https://www.mitpressjournals.org/doi/pdf/10.1162/089892903321107891>
- [28] Gerstner, W., and Kistler, W. M. 2002. *Spiking Neuron Models: Single Neurons, Populations, Plasticity*. Available at: <http://catdir.loc.gov/catdir/samples/cam031/2002067657.pdf>
- [29] Koch, C. *Biophysics of Computation: Information Processing in Single Neurons*. 1999. *Biophysics of Computation: Information Processing in Single Neurons*.
- [30] Izhikevich, E. M. (2007). *Dynamical systems in neuroscience*. MIT press.
- [31] Shiu, P. K., Sterne, G. R., Spiller, N., Franconville, R., Sandoval, A., Zhou, J., ... & Scott, K. (2023). A leaky integrate-and-fire computational model based on the connectome of the entire adult *Drosophila* brain reveals insights into sensorimotor processing. *bioRxiv*.
- [32] Lazar, A. A., Liu, T., Turkcan, M. K., & Zhou, Y. (2021). Accelerating with FlyBrainLab the discovery of the functional logic of the *Drosophila* brain in the connectomic and synaptomic era. *Elife*, 10, e62362.
- [33] Kakaria, K. S., & De Bivort, B. L. (2017). Ring attractor dynamics emerge from a spiking model of the entire protocerebral bridge. *Frontiers in behavioral neuroscience*, 11, 8.

- [34] Churgin, M. A., Lavrentovich, D., Smith, M. A., Gao, R., Boyden, E., & de Bivort, B. (2021). Neural correlates of individual odor preference in *Drosophila*. *bioRxiv*, 2021-12.
- [35] Buhmann, J., Sheridan, A., Malin-Mayor, C., Schlegel, P., Gerhard, S., Kazimiers, T., ... & Funke, J. (2021). Automatic detection of synaptic partners in a whole-brain *Drosophila* electron microscopy data set. *Nature methods*, 18(7), 771-774.
- [36] Dorkenwald, S., McKellar, C. E., Macrina, T., Kemnitz, N., Lee, K., Lu, R., ... & Seung, H. S. (2022). FlyWire: online community for whole-brain connectomics. *Nature methods*, 19(1), 119-128.
- [37] Namiki, S., Dickinson, M. H., Wong, A. M., Korff, W., & Card, G. M. (2018). The functional organization of descending sensory-motor pathways in *Drosophila*. *Elife*, 7, e34272.
- [38] Aso, Y., Sitaraman, D., Ichinose, T., Kaun, K. R., Vogt, K., Belliart-Guérin, G., ... & Rubin, G. M. (2014). Mushroom body output neurons encode valence and guide memory-based action selection in *Drosophila*. *elife*, 3, e04580.
- [39] brian2- <https://brian2.readthedocs.io/en/stable/>
- [40] flywire- <https://flywire.ai/>

PAPER NAME

sharvani_22mslsbf03_plag check2.docx

AUTHOR

Saraboji K

WORD COUNT

4387 Words

CHARACTER COUNT

25326 Characters

PAGE COUNT

32 Pages

FILE SIZE

5.5MB

SUBMISSION DATE

Jun 20, 2024 7:47 AM GMT+5:30

REPORT DATE

Jun 20, 2024 7:48 AM GMT+5:30

● 7% Overall Similarity

The combined total of all matches, including overlapping sources, for each database.

- 3% Internet database
- 6% Publications database
- Crossref database
- Crossref Posted Content database